LAWRENCE
LIVERMORE
NATIONAL
LABORATORY

LLNL-PROC-418369

Transitions of Dislocation Glide to Twinning and Shear Transformation in Shock-Deformed Tantalum

L. L. Hsiung, G. H. Campbell, J. M. McNaney

October 20, 2009

2010 TMS Annual Meeting
Seattle, WA, United States
February 15, 2010 through February 18, 2010

Disclaimer

Transitions of Dislocation Glide to Twinning and Shear Transformation in Shock-Deformed Tantalum

Luke L. Hsiung, Geoffrey H. Campbell, James M. McNaney

Lawrence Livermore National Laboratory
Physical and Life Sciences Directorate
P. O. Box 808, L-352
Livermore, CA 94551-9900

Keywords. Shock deformation, dislocation structure, twinning, shear transformation

Introduction

Recent TEM studies of deformation substructures developed in tantalum and tantalum-tungsten alloys shock-deformed at a peak pressure ~45 GPa have revealed the occurrence of shock-induced phase transformation [i.e., α (bcc) $\rightarrow$ ω (hexagonal) transition] in addition to shock-induced deformation twinning [1, 2]. The volume fraction of twin and ω domains increases with increasing content of tungsten. A controversy arises since tantalum exhibits no clear equilibrium solid-state phase transformation under hydrostatic pressures up to 174 GPa [3-5]. It is known that phase stability of a material system under different temperatures and pressures is determined by system free energy. That is, a structural phase that has the lowest free energy will be stable. For pressure-induced phase transformation under hydrostatic-pressure conditions, tantalum may undergo phase transition when the free energy of a competing phase ω becomes smaller than that of the parent phase α above a critical pressure (P_{eq}), i.e., the equilibrium $\alpha \rightarrow \omega$ transition occurs when the pressure increases above P_{eq}. However, it is also known that material shocked under dynamic pressure can lead to a considerable increase in temperature, and the higher the applied pressure the higher the overheat temperature. This means a higher pressure is required to achieve an equivalent volume (or density) in dynamic-pressure conditions than in hydrostatic-pressure conditions. Accordingly, P_{eq} for $\alpha \rightarrow \omega$ transition is anticipated to increase under dynamic-pressure conditions as a result of the temperature effect. Although no clear equilibrium transition pressure under hydrostatic-pressure conditions is reported for tantalum [3-5], it is reasonable to assume that P_{eq} under dynamic-pressure conditions will be considerably higher than that under hydrostatic-pressure conditions if there is a pressure-induced $\alpha \rightarrow \omega$ transition in tantalum. The observation of $\alpha \rightarrow \omega$ transition in shock-compressed tantalum and tantalum-tungsten alloys at ~45 GPa in fact reveals the occurrence of a non-equilibrium phase transformation at such a low pressure. We therefore postulated that the equation of state (EOS) based on static thermodynamics, which asserts that the system free energy (G) is a function of volume (V), pressure (P), and temperature (T), i.e., G = F(V, P, T) is insufficient to rationalize the system free energy under dynamic-pressure conditions. Since shear deformation was found to play a crucial role in shock-induced deformation twins and ω phase, the density and arrangement of dislocations, which can alter and increase the system free energy, should also be taken into account to rationalize the non-equilibrium phase transformation in shocked tantalum.

Typical arrangements of high-density dislocations formed in pure tantalum shocked at ~45 GPa are shown in Figs. 1a and 1b. Figure 1a reveals a cellular dislocation structure but no twins or ω phase-domains were observed in this region. The formation of low-energy type cellular dislocation structures indicates the occurrence of dynamic-recovery reactions to reduce dislocation density in this region. Figure 1b shows an evenly distributed dislocation structure with a local dislocation density (ρ) as high as ~5 x 10^{12} cm^{-2} according to $\rho \approx 1/l^2$, where l (~4.5 nm) is the spacing between two dislocations. Here shock-induced twin plates and ω phase-domains can be readily seen. These observations provide us a clue that dislocation arrangement and density population, which can alter system free energy through the changes of dislocation self-energy (E_s) and dislocation interaction energy (E_{ij}), are relevant to the occurrence of shock-induced twinning and phase transformation in tantalum. The objective of this paper is to report new results obtained from pure tantalum and tantalum-

tungsten alloys shocked at ~30 GPa in order to clarify the correlation between dislocation structure (i.e., density and arrangement) and shock-induced twinning and $\alpha \rightarrow \omega$ transition. Emphasis is placed especially on the $\alpha \rightarrow \omega$ transition. Physical mechanisms are subsequently proposed to rationalize the shock-induced twinning and non-equilibrium phase transformation.

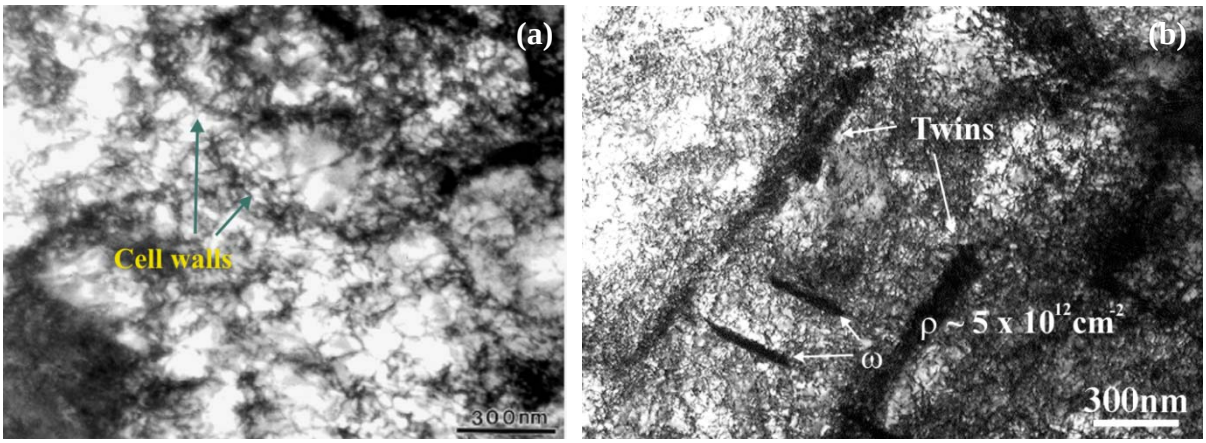

Fig. 1. Bright-field TEM images demonstrate the formation (a) cellular dislocation structure resulting from dynamic recovery reactions and (b) dense and evenly distributed dislocation structure co-exists with twin and ω domains in pure tantalum shocked at 45 GPa.

Experimental

Ingot metallurgy (IM) test materials (commercially pure Ta, Ta-5wt.%W, and Ta-10 wt.%W) in the form of plate stock produced using a standard electron-beam melting process were obtained from Cabot Corporation, Boyertown, PA. Details of explosively driven shock-recovery experiment used for this investigation can be found in [6]. Single explosively driven shock-recovery experiments were conducted by detonating explosive on hemisphere-shaped alloy plates (~3mm thick) that were shocked into polyurethane foams immersed in a water tank. The shock experiments were carried out under a peak pressure of ~30GPa simulated using a CALE continuum hydrodynamic code [7]. Thin foils for TEM analysis were prepared by a standard procedure that includes slicing, grinding, and polishing the recovered fragments with the foils surface approximately perpendicular to the loading axis. Final thinning of the foils was performed using a standard twin-jet electropolishing technique in an electrolyte (94 vol.% methanol, 5 vol.% sulfuric acid and 1 vol.% hydrofluoric acid) at ~25 V and -20 $^{\circ}$C. The microstructures of shock-recovered fragments were then characterized using a JEOL 200CX transmission electron microscope (TEM). A software package CaRIne Crystallography 3.1 was used to simulate electron diffraction patterns in order to identify shock-induced ω phase.

Results and Discussion

Shock-induced microstructures

Figures 2a and 2b are bright-field TEM images showing dislocation tangling and cellular dislocation structures resulting from dynamic recovery reactions were formed in shocked pure Ta and Ta-5W samples. No twin domain or ω phase was found in shocked pure Ta and Ta-5W samples. The dislocation structure formed in shocked Ta-10W is however very different. As can be seen in Fig. 3, dislocation lines are denser and evenly distributed, and some ω domains with a diffraction pattern of the $[10\bar{1}0]_{\omega}$ zone were readily observed. Details on the identification of omega phase will be discussed below. The local dislocation density in Fig. 3 is estimated to be on the order of 2 x 10^{12} cm^{-2} according to $\rho \approx 1/l^2$, where l (~6 nm) is the spacing between two dislocations. Since the major effect of W addition is to impede dislocation motion, i.e., to reduce dislocation mobility in order to strengthen tantalum, these observations indicates that the dynamic recovery reactions to form cellular structure are largely suppressed in Ta-10W shocked under the same pressure as a result of reduced dislocation mobility.

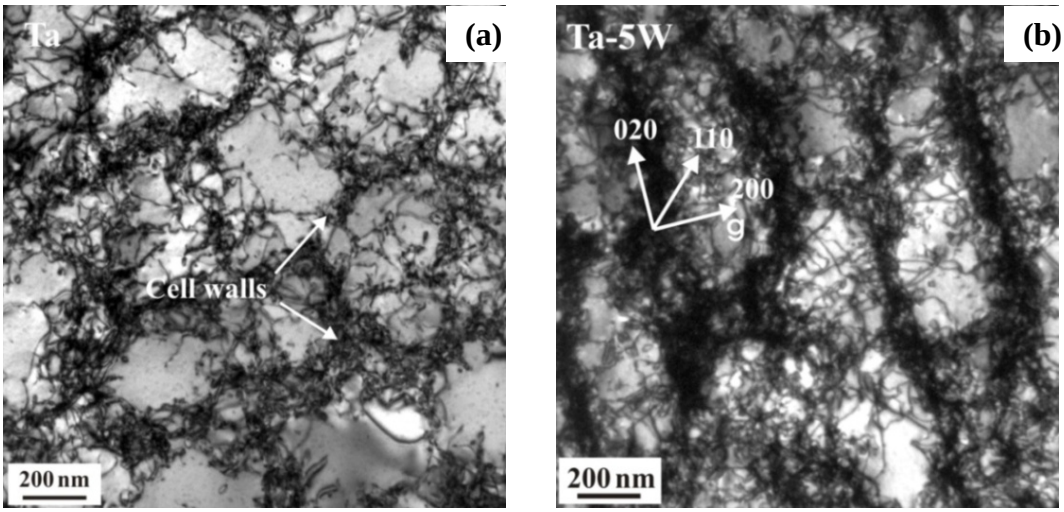

Fig. 2. Bright-field TEM images demonstrate cellular dislocation structures formed in (a) shock-recovered pure Ta, and (b) shock-recovered Ta-5W. Note that the images were taken from the [001]-oriented grains.

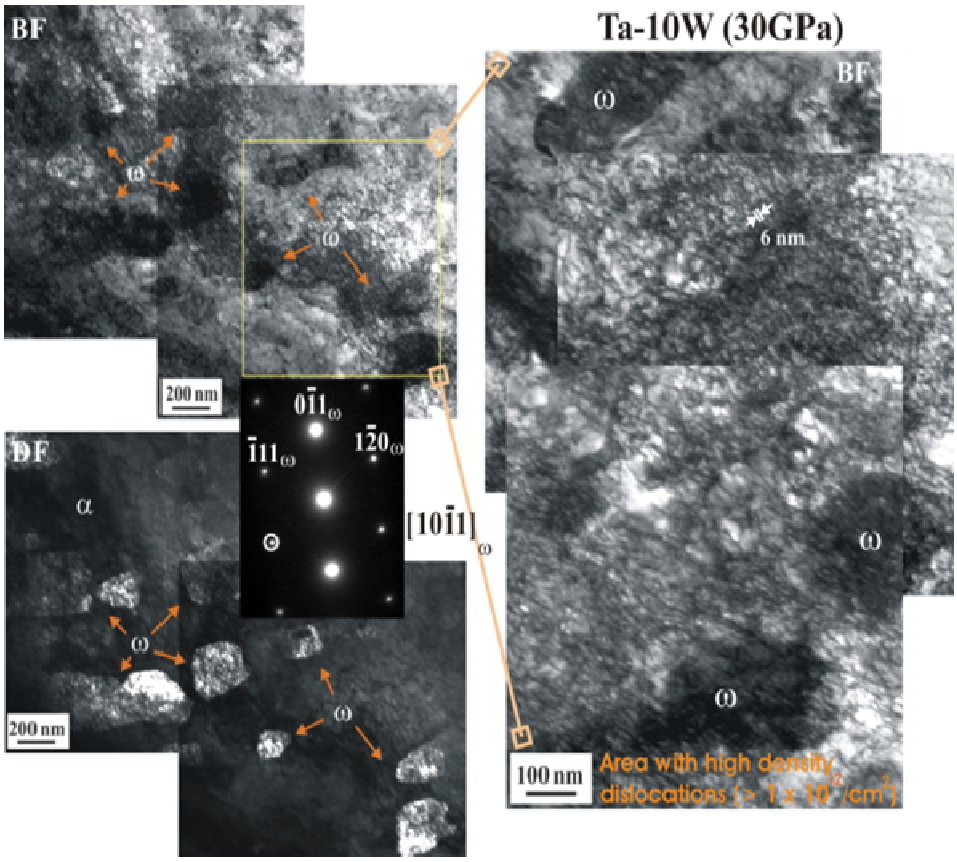

Fig. 3. Bright-field and dark-field TEM images reveal ω phase domains embedded in dense and evenly distributed dislocation arrays in shocked Ta-10W. The inset selected-area diffraction pattern is of the $[10\bar{1}1]_\omega$-zone.

Crystal structure of ω phase

It is known that the ω (hexagonal)-lattice can be perceived by collapsing one pair of (111) planes within the α (bcc)-lattice and leaving the adjacent (111) planes unaltered [8]. The atomic displacements required are $\pm a_o\sqrt{3}/12$, where a_o is the lattice parameter of α-lattice. It contains 3-atoms/unit cell with the lattice constants: $a_\omega = \sqrt{2}\ a_o = 0.468$ nm and $c_\omega = (\sqrt{3}/2)\ a_o = 0.286$ nm ($c_\omega/a_\omega = 0.611$). There is no volume change associated with this transformation. The atomic positions are a: (0,0,0); b: (2/3,1/3,1/2); c: (1/3,2/3,1/2). However, when we carefully examined the atomic positions of the hexagonal lattice, we find that the distance (0.27 nm) is too short to accommodate atoms b and c with the atomic diameter equivalent to c_ω (0.286 nm), as shown in Fig. 4a. These two atoms have to shuffle slightly so as to increase the distance to ~0.302 nm, as shown in Fig. 4b. The atomic shuffling does not alter the lattice constants but results in a psudo-hexagonal structure due to the loss of six-fold symmetry. The atomic positions of the psudo-hexagonal lattice thus become a: (0,0,0); b: (0.685, 0.315, 0.5); c: (0.315, 0.685, 0.5). We accordingly identified the existence of ω phase in shock-recovered Ta-10W based upon the hexagonal and pseudo-hexagonal structures of ω phase by comparing and matching the observed and simulated diffraction patterns, as demonstrated in Fig. 5. Here, the formation of ω phase can be easily recognized from the appearance of extra spots excited at various 1/3<112> and 2/3<112> positions in the $[0\bar{1}1]$-, [012]-, and [113]-zone diffraction patterns of α phase, in which the simulated $[11\bar{2}0]$-, $[11\bar{2}6]$-, and $[11\bar{2}3]$-zone patterns of both ideal-hexagonal and pseudo-hexagonal ω phase are displayed at the right hand side of Fig. 5. The simulated patterns of pseudo-hexagonal structure match very well with the observed diffraction patterns. These results confirm that the crystal structure of shock-induced ω phase is not ideal hexagonal but pseudo-hexagonal as explained and illustrated in Fig. 4. In addition, the results reveal that the α and ω phases have the following orientation relationships: (a) $\{2\bar{1}1\} \parallel (\bar{1}100)$, <011> ‖ $[11\bar{2}0]$; (b) {100} ‖ $(0\bar{2}21)$, <012> ‖ $[11\bar{2}6]$; (c) $\{01\bar{1}\} \parallel (0\bar{1}11)$, <113> ‖ $[11\bar{2}3]$.

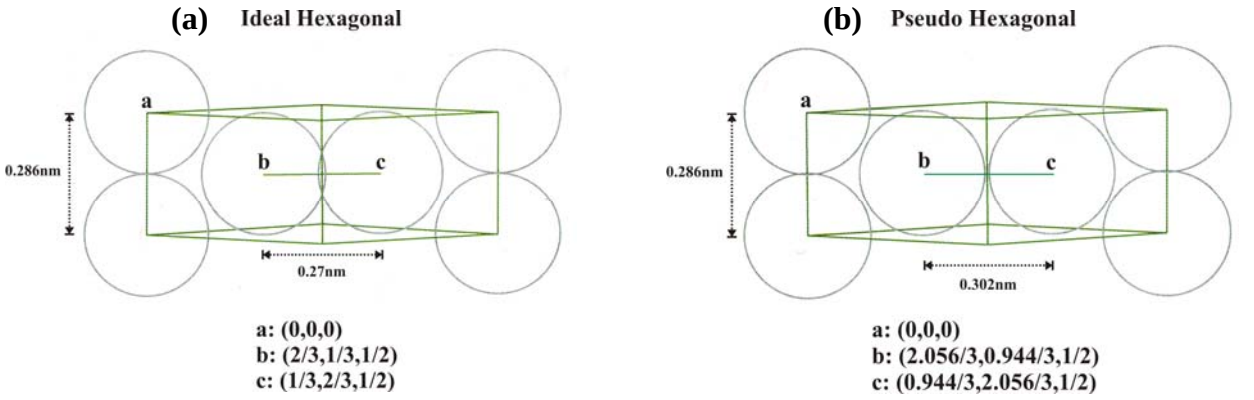

Fig. 4. Schematic illustrations demonstrate the atomic positions of (a) ideal hexagonal ω-lattice, and (b) pseudo hexagonal ω-lattice. See text for explanation.

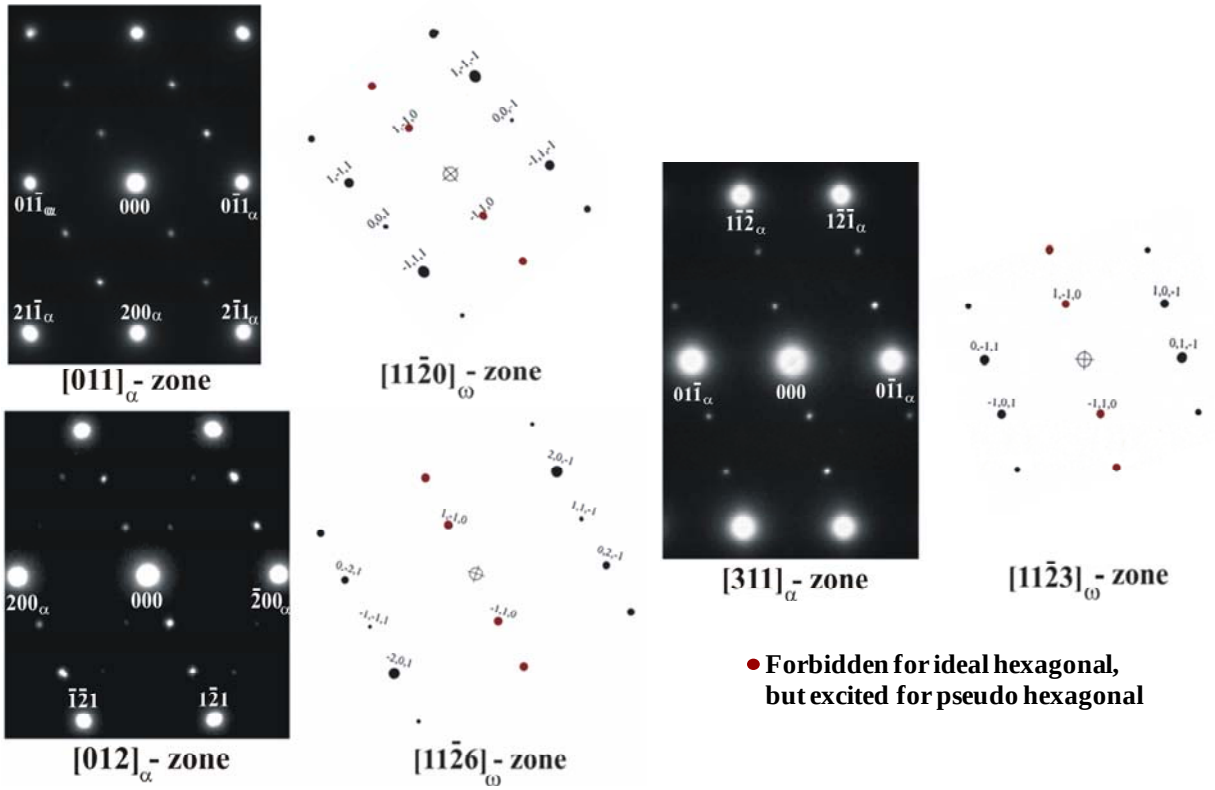

Fig. 5. The selected-area diffraction patterns of $[0\bar{1}1]$-, [012]-, and $[1\bar{1}3]$-zone of α phase in association of weak diffraction spots generated from ω phase. The simulated $[11\bar{2}0]$-, $[11\bar{2}6]$-, and $[11\bar{2}3]$-zone patterns of ω phase are also displayed.

Proposed mechanisms for twinning and α → ω transition

It was proposed previously in [2] that similar to the shear mechanism for deformation twinning, i.e., homogeneous 1/6<111> shear in consecutive $\{211\}_\alpha$ planes, the α → ω transition can take place through the inhomogeneous shear of $1/12\langle 1\bar{1}\bar{1}\rangle$, $1/3\langle 1\bar{1}\bar{1}\rangle$, and $1/12\langle 1\bar{1}\bar{1}\rangle$ in consecutive $\{211\}_\alpha$ planes, as illustrated in Fig. 6a. The stacking sequence resulting from the three-layer inhomogeneous shear is literally equivalent to the atomic shuffling of $\pm 1/12[1\bar{1}\bar{1}]$ in a pair of {211} planes for the α→ ω transition according to the collapse model mentioned above. The shock-induced α → ω transition in tantalum can thus be regarded as a diffusionless shear transformation. The shock-induced twinning and α → ω transition in association with dense and evenly distributed dislocation structure may imply that both twinning and α → ω transition are alternative deformation mechanisms to accommodate insufficient dislocation flow resulting from the exhaustion of dislocation sources when dynamic recovery reactions for dislocation annihilation and cellular dislocation structures become largely suppressed. The shear operations for the transition of bcc structure to twin and ω domains can be produced by the glide of partial dislocations of the type *1/3*<111>, *1/6*<111> and *1/12*<111> dissociated from the ½<111> perfect dislocation, as illustrated in Fig. 6b. Each ½<111> dislocation can dissociate into three *1/6*<111> partials (each one plane apart) in the {211} plane to form a three-layered twin domain. In other words, it requires the dissociation of two ½<111> dislocations with three-plane separation (0.405 nm) to form a unit (six-layer) twin domain. Similarly, the partial dislocations for the α → ω transition can be obtained by the dissociation of two ½<111> dislocations with six-plane separation (0.81 nm) into two *1/12*<111> partials and one *1/3*<111> partial (each one plane apart) in the {211} plane to form a unit (six-layer) ω domain. These two dissociation reactions, i.e. $\mathbf{b} \rightarrow \mathbf{b}_1 + \mathbf{b}_2 + \mathbf{b}_3$, are energetically feasible because the

free energy is gained in the dissociation process according to Frank's rule [9]: $b_1^2 + b_2^2 + b_3^2 < b^2$. The next question is then how these dislocation dissociations are abundant enough to overcome the energy barriers required for nucleating twin and/or ω domains with a finite size greater than a critical thickness? To answer this question, we will need to know the interfacial energies for twin and ω domains and the change of chemical energy for the α → ω transition, but it is more important for now to evaluate the threshold stresses and the critical densities of evenly distributed dislocations required to trigger the transitions of one-dimensional line defect to three-dimensional phase domain. The transitions may be feasible to occur through the occurrence of a dislocation clustering reaction in {211} with ½[111] dislocations three-plane separation (0.405 nm) for twinning and six-plane separation (0.81 nm) for α → ω transition, which are proposed and described below.

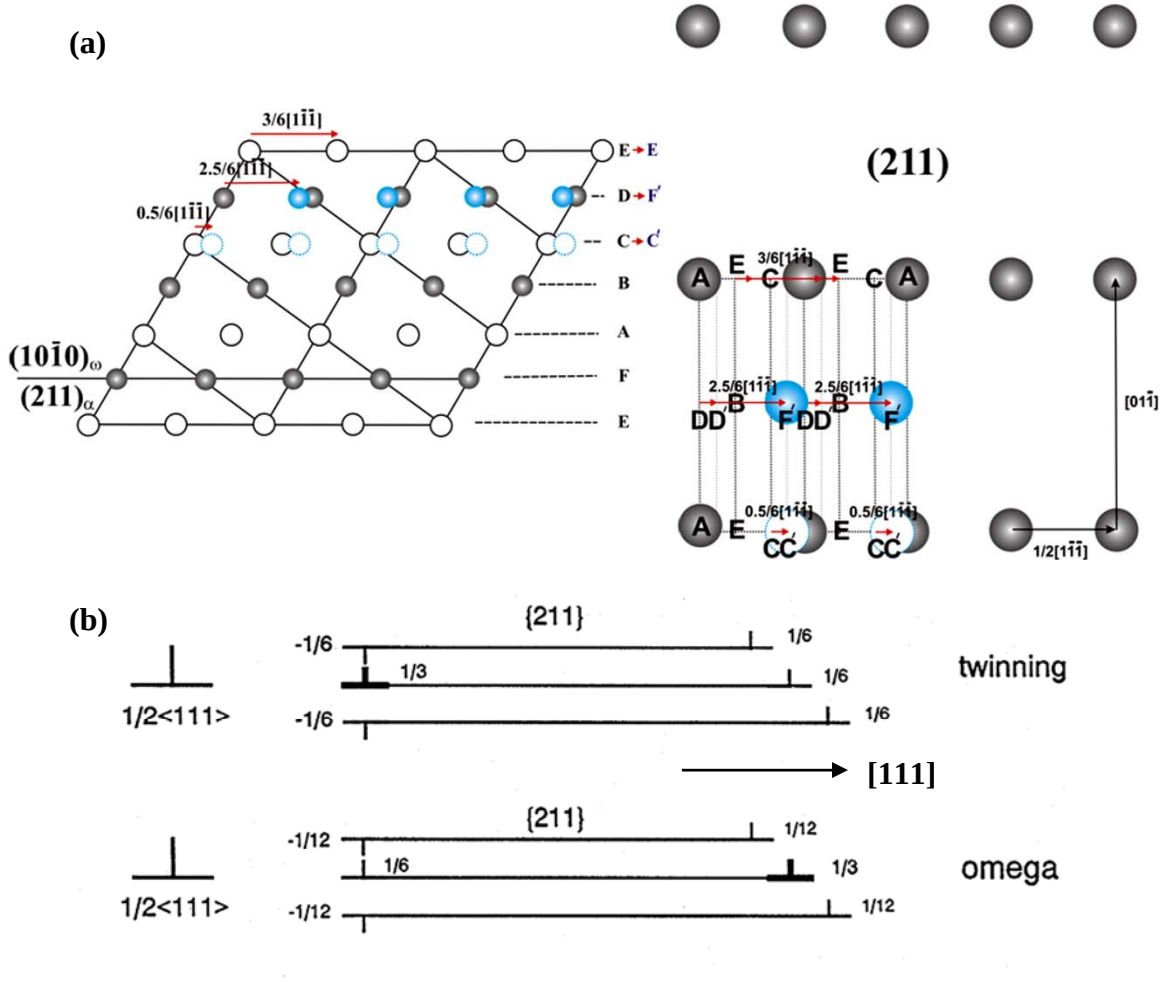

Fig. 6. Schematic illustrations demonstrate (a) the α → ω transition can take place through inhomogeneous shear on the {211} plane viewing from the $[0\bar{1}1]$ and [211] directions; (b) the dissociation of ½ <111> dislocation for the reactions of twinning and omega transition.

Threshold stresses for twinning and $\alpha \rightarrow \omega$ shear trnsformation

The threshold stresses and critical dislocation densities for the transitions of dislocation glide to twinning and shear transformation can be evaluated by considering a competing process between a Frank-Read dislocation source and a dislocation clustering source generated from a jogged screw dislocation. Figures 7a and 7b

illustrate a Frank-Read dislocation source in a dense screw dislocation array and critical spacing of the dislocation array to cause the exhaustion of Frank-Read source. Here, the shear stress ($\tau_{F.R.}$) to operate Frank-Read source is expressed as $\tau_{F.R.} = \frac{2\alpha\mu b}{\lambda}$, where α = 0.25 ~ 0.5, μ (62.8 GPa [10]) is shear modulus, λ is the length of free segment between two pinning points, and b (0.286 nm) is the magnitude of Burgers vector. The repulsive stress between bowing segment and adjacent dislocation segment will make a distance ($\delta = 0.073\alpha\lambda$) between the two dislocation segments. Thus, the F-R dislocation source is operative when $\lambda > \frac{2\alpha}{\alpha+0.15} l$, where l is the average dislocation spacing. However, the F-R dislocation source becomes inoperative when $\lambda \leq \frac{2\alpha}{\alpha+0.15} l$, but the two edge dislocation segments can still glide in the opposite <111> directions. The operation of solely edge dislocation segments is the key to form a dislocation clustering source, as illustrated in Fig. 8. Here two dislocation loops separated by a jog height (d) are expanding solely by the movement of edge segments. It becomes a twinning source when d = $3d_{211}$ = 0.405 nm and a shear transformation source when d = $6d_{211}$ = 0.81 nm. It is noted that a screw dislocation line in reality contains numerous jogs with different heights, which can either be preexisting thermal jogs or generated from the intersection of dislocation lines during deformation generated from a jogged screw dislocation. Thus, the threshold stress (τ_c) for twinning or shear transformation is in fact the stress required to overcome the attractive force between two edge segments with an opposite sign (i.e., edge dipole), which is given as $\tau_c = \frac{\mu b}{8\pi(1-\upsilon)d}$ [10], and ν = 0.43 for Ta [10]. Thus, τ_c (twin) = 2.81 GPa, and τ_c (ω) = 1.41 GPa. Transitions from dislocation glide to twinning and/or shear transformation occur when $\tau_{F.R.}$ is greater than τ_c (twin) and/or τ_c (ω) at local region. The critical dislocation densities ($\rho_c = {}^{1}/_{l^2}, and\ l = \frac{(\alpha+0.15)\lambda}{2\alpha}$) for the transitions can therefore be evaluated by setting $\tau_{F.R.} = \tau_c$ (twin) and/or τ_c (ω). Depending on the value of α (0.25 ~ 0.5), ρ_c (twinning) is in a range between 6.0 x 10^{12} cm^{-2} (α = 0.5) and 1.6 x 10^{13} cm^{-2} (α = 0.25), whereas ρ_c (ω) is in a range between 1.5 x 10^{12} cm^{-2} (α = 0.5) and 4.0 x 10^{12} cm^{-2} (α = 0.25). These results indicate that the transitions of dislocation glide to twinning and/or shear transformation in tantalum are likely to occur when the local density of evenly distributed dislocations reaches to the range of 2.0 x 10^{12} cm^{-2} ~ 2.0 x 10^{13} cm^{-2}, which is fairly consistent with observations.

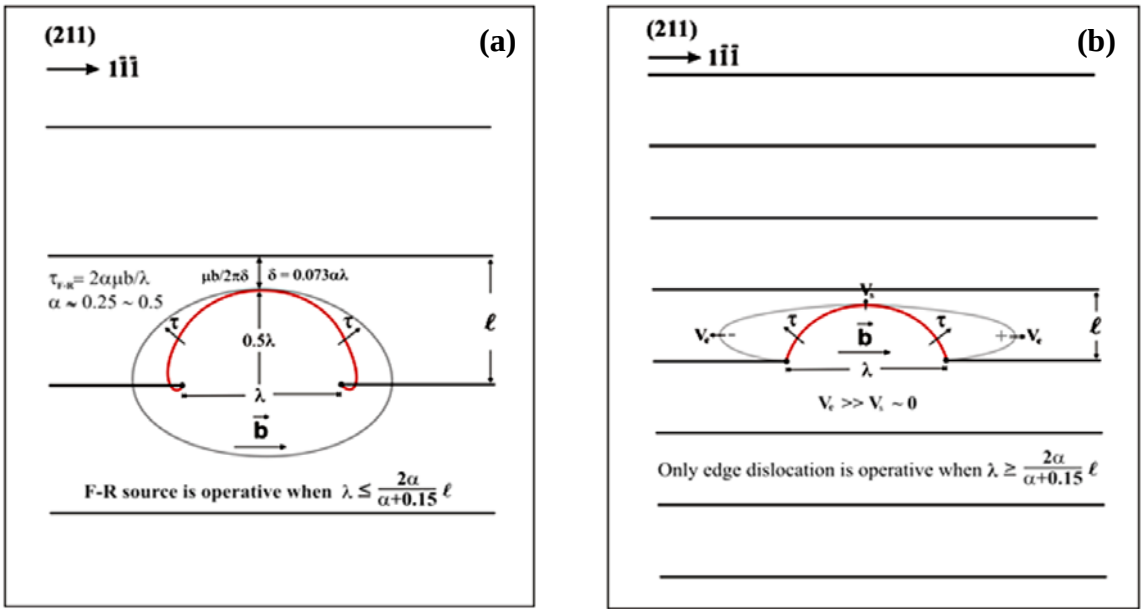

Fig. 7. Schematic illustrations of (a) Frank-Read dislocation source in an evenly distributed dislocation array, and (b) a critical geometry where Frank-Read dislocation source becomes exhausted in an evenly distributed dislocation array. See text for explanation.

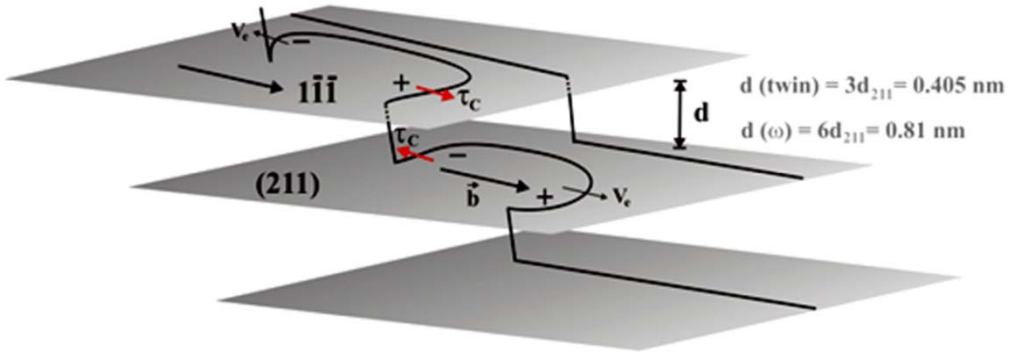

Fig. 8. A schematic illustration of a dislocation clustering source resulting from the movement of edge dislocation segments of a jogged dislocation for twinning and shear transformation.

Summary

Shock-induced twinning and $\alpha \rightarrow \omega$ transition in tantalum and tantalum-tungsten alloys have been further investigated through single explosively driven shock-recovery experiments conducted by detonating explosive on hemisphere-shaped alloy plates to generate a peak pressure ~30 GPa. The onset of twinning and $\alpha \rightarrow \omega$ transition is found to be intimately related to the density and arrangement of dislocation structure. While no twins or ω phase domains were found in pure Ta and Ta-5W samples that contain mainly low-density cellular structures, shock-induced ω phase domains were found in Ta-10W sample that contains evenly-distributed dislocation arrays with a density greater than 1 x 10^{12} cm^{-2} measured based on $\rho \approx 1/l^2$, where l is the spacing between two dislocations. The structure of shock-induced ω phase is identified to be pseudo hexagonal. It is suggested that shear deformation in {211} is the major cause for the formation of shock-induced twin and ω phase domains. Heterogeneous nucleation mechanisms based on the competition between Frank-Read dislocation source and dislocation clustering source generated from a jogged screw dislocation in association with the core dissociation of ½<111> into three *1/6*<111> twinning dislocations, and *1/12*<111>, *1/3*<111> and *1/12*<111> transformation dislocations are proposed. Threshold stresses ranging between 1.41 ~ 2.81 GPa and critical dislocation densities ranging between 2 x 10^{12} ~ 2 x 10^{13} cm^{-2} are accordingly assessed for the transitions of dislocation glide to twinning and shear transformation in shock-deformed tantalum.

Acknowledgements

This work was performed under the auspices of the U.S. Department of Energy by Lawrence Livermore National Laboratory under Contract DE-AC52-07NA27344.

Reference

1. L.M. Hsiung and D.H. Lassila, Scripta Mater. **39**, 603 (1998).
2. L.M. Hsiung and D.H. Lassila, Acta Mater. **48**, 4851 (2000).
3. D.A. Young, Phase Diagrams of the Elements, University of California Press, Berkeley: California (1991).
4. E. Yu Tonkov, E.G. Ponyatovsky, Phase Transformations of Elements under High Pressure, CRC Press, 239 (2005).
5. H. Cynn, C.S. Yoo, Equation of state of tantalum to 174 GPa, Phys. Rev. B, **59**, 8526 (1999).
6. G.H. Campbell, G.C. Archbold, O.A. Hurricane, and P. L. Miller, J. of Appl. Phys. **101**, 033540 (2007).
7. R.T. Barton, in *Numerical Astrophysics*, edited by J.M. Centrella, J.M. LeBlanc, and R.L. Bowers (Jones and Bartlett, Boston, 1985), 482.
8. S. K. Zikka, Y. K. Vohra, and R. Chidambaram, *Progress in Materials Science* **27**, 245 (1982).
9. J. Wertman, J.R. Wertman, *Elementary Dislocation Theory*, Macmillan (1964).
10. E.M. Nadgornyi, *Progress in Materials Science* **31**, 1 (1988).